Voltage Source Power Line Conditioner for Applications in Local Supply Systems

Ryszard Strzelecki
Faculty of Electrical and Control Engineering
Gdańsk University of Technology
Gdańsk, Poland
ryszard.strzelecki@pg.edu.pl

Natalia Strzelecka
Faculty of Electrical Engineering
Gdynia Maritime University
Gdynia, Poland
n.strzelecka@we.umg.edu.pl

Abstract— **The paper presents the basic principles of operation of voltage source power line conditioners (VSPLC) as well as their energy and filtration properties. A 4-level cascade based Voltage Source Converter (VSC) is used as a voltage source. The advantages of this topology is relatively simple construction and simple way of balanced DC link voltages. Results of the theoretical and experimental investigations confirm good energetic and filtration properties compared to Active Power Filters (APF).**

Keywords—power electronics, power factor correction, active power conditioner, blocking harmonics of the load current, power flow control, multilevel source converter

I. INTRODUCTION

The literature suggests that isolation of disturbance sources due to introduction of the nonlinear loads can be realized in many different ways. For instance, one can use "traditional" pure or hybrid APF [1,2,3]. In this case, compensatory components must be extracted from the measured load currents or source. The quality of filtration corresponds with the accuracy of isolating the components of distorted currents that are interesting to us.

The paper, at hand illustrates a different way to obtain sinusoidal source currents. In this approach one must focus on controlling the parallel inverter as a voltage generator and adjust the angle of this voltage in relation to the source of voltage. In that way sinusoidal source current can be sustained. The major difference between the proposed conditioner and alternative solutions is about the compensation of the higher harmonics. For the solution proposed in this paper, there is no need to detect the load current harmonics, because they are naturally absorbed by the VSC. The VSC "isolates" load from supply system [4,5,6].

Other advantages of the proposed solution include:
- simple control algorithm;
- filtration quality independent from wave shape of the load current;
- where control algorithm is equipped with additional filters, filtration quality is independent from shape of the network voltage wave;

Some disadvantages include:
- input power factor is changing (slightly) with load power factor and power absorbed by the load;
- possible troubles in turn on mode.

II. VPLC - PRINCIPLE OF OPERATION VSPLC

Fig. 1 presents a scheme of the proposed VSPLC (a), an vector diagram of currents and voltages (b) corresponding to the steady state operation of the system and basic control algorithm (c) implemented in system with sinusoidal network voltage u_S. VPLC consists of two major elements: series

impedance Z_S and controlled the synchronous sinusoidal voltage source u_V inserted in parallel between the supply and the load.

Potential for power flow from supply to load exists with voltage u_V, produced by the converter, i_S shifted with angle γ_0, in relation to voltage u_S [7]. Moreover, with sinusoidal network voltage u_S and sinusoidal inverter's output voltage u_V with the same amplitude u_S, the source current i_S also becomes sinusoidal. Voltage on source element of the inverter can be controlled by changing γ_0 angle. But there is a disadvantage of this solution. Input power factor changes (in slightly degree) correspond with power factor and/or power absorbed by the load .
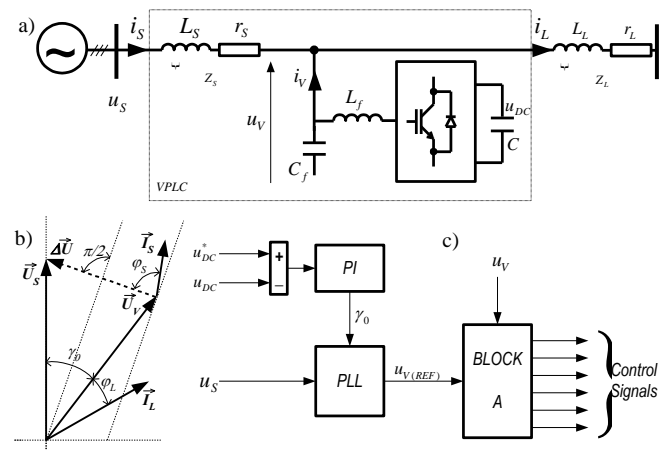

Fig. 1. Investigated VSPLC system: scheme (a), vector diagram (b), basic control algorithm (c)

Basic control algorithm (Fig.1c) PLL generates signal $u_{V(REF)}$ with frequency equal to that of the network and phase shifted in relation to u_S with angle γ_0. Block A stabilizes voltage on the load at the reference value by means of a closed-loop control error between RMS u_V and reference voltage $u_{V(REF)}$. PI controller was implemented to keep constant value of the total DC link voltage . PI controller is implemented to maintain constant value of the voltage U_{DC}, of which input signal equals the difference between reference voltage U^*_{DC} and actual measured voltage U_{DC}. Fig. 2 illustrates the operation of the VSPLC system controlled by the basic algorithm illustrates the currents and voltages .

Situation gets more complex when network voltage u_S is unsinusoidal (poses higher harmonics or/and non-periodic components). In this case the control algorithm must be equipped with additional filter (Fig.3).

The filter should extract all the unneeded components (higher harmonics and non-periodic) from distorted network voltage u_{Sd}. Then only the basic component of the network
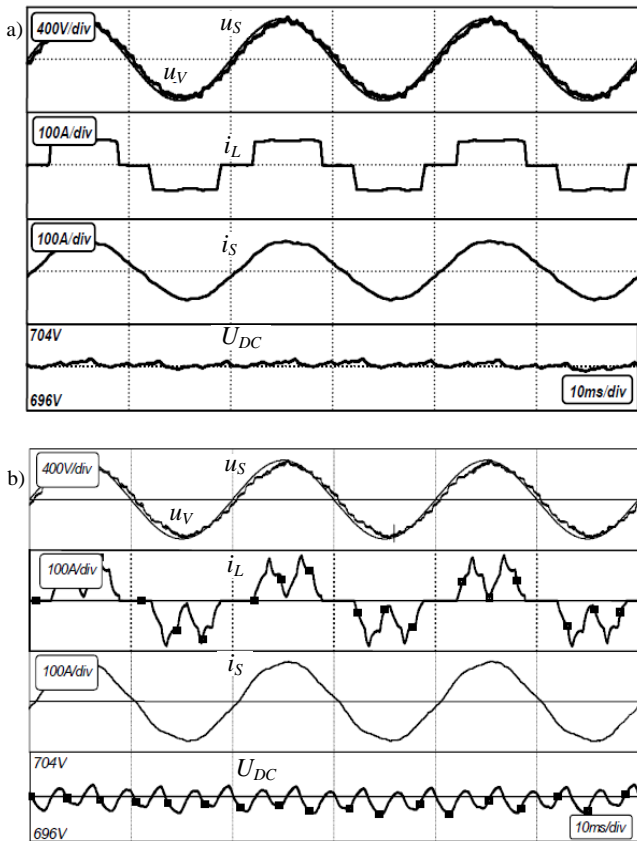
Fig. 2. VSPLC system operation with basic control algorithm and diode rectifier load, with: RL(a) and RC (b) output
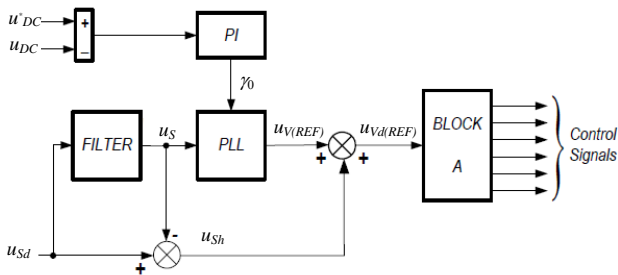

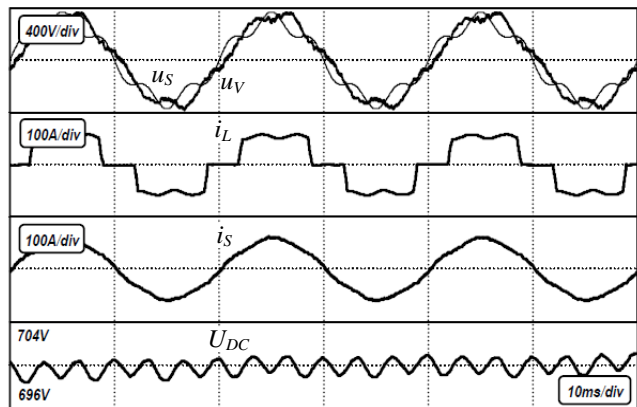Fig. 3. Control algorithm equipped with low-pass filter

Fig. 4. VSPLC system operation when control algorithm is equipped with Chebyshev filter

voltage u_S (at frequency 50 Hz) has to be shifted with angle γ_0. To obrain sinusoidal network current i_S one must include voltage distortion components u_{Sh} in shifted voltage $u_{V(REF)}$

and shaping voltage $u_{Vd(REF)}$. Fig.4 presents of the simulation results with network voltage distorted of 20% 5th harmonic. 3rd rank Chebyshev filter was used to extract distortions [8].

III. ENERGETIC AND FILTRATION PROPERTIES OF VSPLC

This section compares energetic properties of the classic APFs with VSPLCs. On the basis of the vector graph from Fig.1, following dependencies can be determined:

$$\vec{U}_S = U, \qquad \vec{U}_V = \vec{U}_L = U \cdot e^{-j\gamma_0},$$

$$\Delta\vec{U}_V = 2 \cdot U \cdot \sin\frac{\gamma_0}{2} \cdot e^{-j(\pi-\gamma_0)/2} \qquad (1)$$

$$\vec{I}_S = \frac{2 \cdot U}{|Z_S|} \cdot \sin\frac{\gamma_0}{2} \cdot e^{-j(\pi-\gamma_0-2\varphi_S)/2},$$

$$\vec{I}_L == \frac{U}{|Z_S|} \cdot e^{-j(\gamma_0+\varphi_L)/2} \qquad (2)$$

where: $\varphi_S = \arctan\frac{\omega L_S}{r_S}$, $\varphi_L = \arctan\frac{\omega L_L}{r_L}$, $U = U_m/\sqrt{2}$, $|Z_S| = \sqrt{(\omega L_S)^2 + r_S^2}$, $|Z_L| = \sqrt{(\omega L_L)^2 + R_L^2}$, U_m – amplitude.

Active P_V, reactive Q_V and distortion D_V powers of the voltage source u_V, are as follows:

$$P_V = U^2\left[\frac{\sin\varphi_S \cdot \sin\gamma_0 - \cos\varphi_S \cdot (1-\cos\gamma_0)}{|Z_S|} - \frac{\cos\varphi_L}{|Z_S|}\right]_{r_S\to0}$$

$$\approx \approx U^2\left(\frac{\sin\gamma_0}{\omega L_S} - \frac{\cos\varphi_L}{|Z_S|}\right) \qquad (3)$$

$$Q_V = U^2\left[\frac{\sin\varphi_S \cdot (1-\cos\gamma_0) + \cos\varphi_S \cdot \sin\gamma_0}{|Z_S|} + \frac{\sin\varphi_L}{|Z_S|}\right]_{r_S\to0} \approx$$

$$\approx U^2\left(\frac{1-\cos\gamma_0}{\omega L_S} + \frac{\sin\varphi_L}{|Z_S|}\right) \qquad (4)$$

$$D_V = U \cdot \sqrt{\sum_{k=2}^{\infty} I_{L(k)}^2} = \sqrt{\sum_{k=2}^{\infty}\left(U \cdot I_{L(k)}\right)^2} = \sqrt{\sum_{k=2}^{\infty} D_{L(k)}^2} \qquad (5)$$

where: Z_L, Z_S –load and supply impedances respectively; $I_{L(k)}$, $D_{L(k)}$ –k^{th} harmonic in load current (RMS value) and distortion power of the load related to k^{th} harmonic respectively.

Taking into consideration equations (4) and (5), the assumption that both VSPLC and APF are perfect compensators what means $D_V = D_L$ and $Q_V = Q_L$, and the fact that during steady states $P_V=0$, the apparent power of the synchronous voltage source u_V in VSPLC can be calculate as follows:

$$S_{V(VSPLC)_{r_S\to0}} \approx$$

$$\approx \sqrt{\left(\frac{P_{max}}{P_L} - \sqrt{\left(\frac{P_{max}}{P_L}\right)^2 - 1} + \tan\varphi_L\right)^2 + \left(\frac{THD(I_L)}{\cos\varphi_L}\right)^2}$$

$$\xrightarrow{\frac{P_{max}}{P_L}\ll1} \sqrt{Q_L^2 + D_L^2} \qquad (6)$$

where: $P_L = (U^2/|Z_L|) \cdot \cos\varphi_L$ – active power of the load; $Q_L = (U^2/|Z_L|) \cdot \sin\varphi_L$ – reactive power of the load; $P_{max} = (U^2/\omega L_S)$ – short circuit power; $TDH(I_L)$ – total harmonic distortion of the load current; $I_{L(1)}$ – RMS value of the 1st harmonic of load current, and $\sum_{k=2}^{\infty} I_{L(k)}^2 = I_{L(1)}^2 \cdot THD^2(I_L)$.

When APF is responsible for compensating of the higher harmonics of load current and load reactive power Q_L, voltage produced by the ideal voltage source, which forces to flow through the parallel coupling inductance L'_S compensating current, is:

$$U_{V(APF)} = \sqrt{(U + \Delta U)^2 + U_h^2} \qquad (7)$$

where: $\Delta U = \omega L'_S \cdot I_{L(1)} \sin \varphi_L = \omega L'_S \cdot P_L/(U \cos \varphi_L) \cdot \sin \varphi_L = L'_S \cdot (P_L/U) \tan \varphi_L$ – voltage drop on the coupling inductance L'_S caused by the component in the compensating current responsible for load reactive power Q_L compensation; $U_h = \sqrt{\sum_{k=2}^{\infty} (k \cdot \omega L'_S \cdot I_{L(k)})^2}$ – voltage drop on the coupling inductance L'_S due to the component in the compensating current that is responsible for higher harmonics in load current $I_{L(k)}$ compensation.

Considering the 6-pulse controlled rectifier as the nonlinear load, voltage U_h could be defined as follows:

$$U_h = \sqrt{\sum_{k=2}^{\infty} \left(k \cdot \omega L'_S \cdot \frac{I_{L(1)}}{k}\right)^2} = \omega L'_S \cdot \frac{P_L}{U \cdot \cos \varphi_L} \cdot \sqrt{N} \qquad (8)$$

where: $I_{L(k)} = I_{L(1)}/k$, N – number of the compensated higher harmonics. Thus equation 7 can be saved in the form:

$$U_{V(APF)} = U \sqrt{\left(1 + \frac{P_L}{P'_{max}} \tan \varphi_L\right)^2 + \left(\frac{P_L}{P'_{max}} \cdot \frac{1}{\cos \varphi_L}\right)^2} \qquad (9)$$

$$I_{V(APF)} = \frac{P_L}{U \cdot \cos \varphi_L} \sqrt{\sin^2 \varphi_L + THD^2(I_L)} \qquad (10)$$

where: $P'_{max} = (U^2/\omega L'_S)$ - maximum active power transmittable through coupling inductance L'_S active power.

After transformation, the apparent power of the voltage source in APF is calculated :

$$S_{V(APF)} =$$
$$= \frac{P_L}{\cos \varphi_L} \sqrt{\left[\left(1 + \frac{P_L}{P'_{max}} \tan \varphi_L\right)^2 + \left(\frac{P_L}{P'_{max}} \cdot \frac{1}{\cos \varphi_L}\right)^2 \cdot N\right] \cdot}$$
$$\cdot \sqrt{\left(\sin^2 \varphi_L + THD^2(I_L)\right)} \xrightarrow[\frac{P'_{max}}{P_L} \gg 1]{} \sqrt{Q_L^2 + D_L^2} \qquad (11)$$

Finally, relation between VSPLC's and APF's apparent powers is calculated by the following equation:

$$\frac{S_{V(SVPLC)}}{S_{V(APF)}} =$$
$$= \frac{\varepsilon' \cdot \cos \varphi_L \cdot \sqrt{\cos^2 \varphi_L \cdot \left(\varepsilon - \sqrt{\varepsilon^2 - 1} + \tan \varphi_L\right)^2 + THD^2(I_L)}}{\sqrt{[\cos^2 \varphi_L \cdot (\varepsilon' + \tan \varphi_L)^2 + N] \cdot [\cos^2 \varphi_L + THD^2(I_L)]}}$$
$$\xrightarrow[\frac{P'_{max}}{P_L} \gg 1, \frac{P_{max}}{P_L} \gg 1]{} 1 \qquad (12)$$

where: $\varepsilon = P_{max}/P_L$ (for VSPLC) , $\varepsilon' = P'_{max}/P'_L$ (for APF)

Fig.5 illustrates theoretical curves based on the equation (12) for different φ_L and $THD(I_L)$. The apparent power of the synchronous voltage source in VPLC, when compared with the apparent power of the synchronous voltage source in

APF, is smaller for greater deformations in the load current and for greater values of φ_L. This is true, because VPLC generates reactive power, and in case of small φ_L and large loads (small value of the $\varepsilon = P_{max}/P_L$ coefficient) the eactive power can be considerably larger than reactive power of the load.
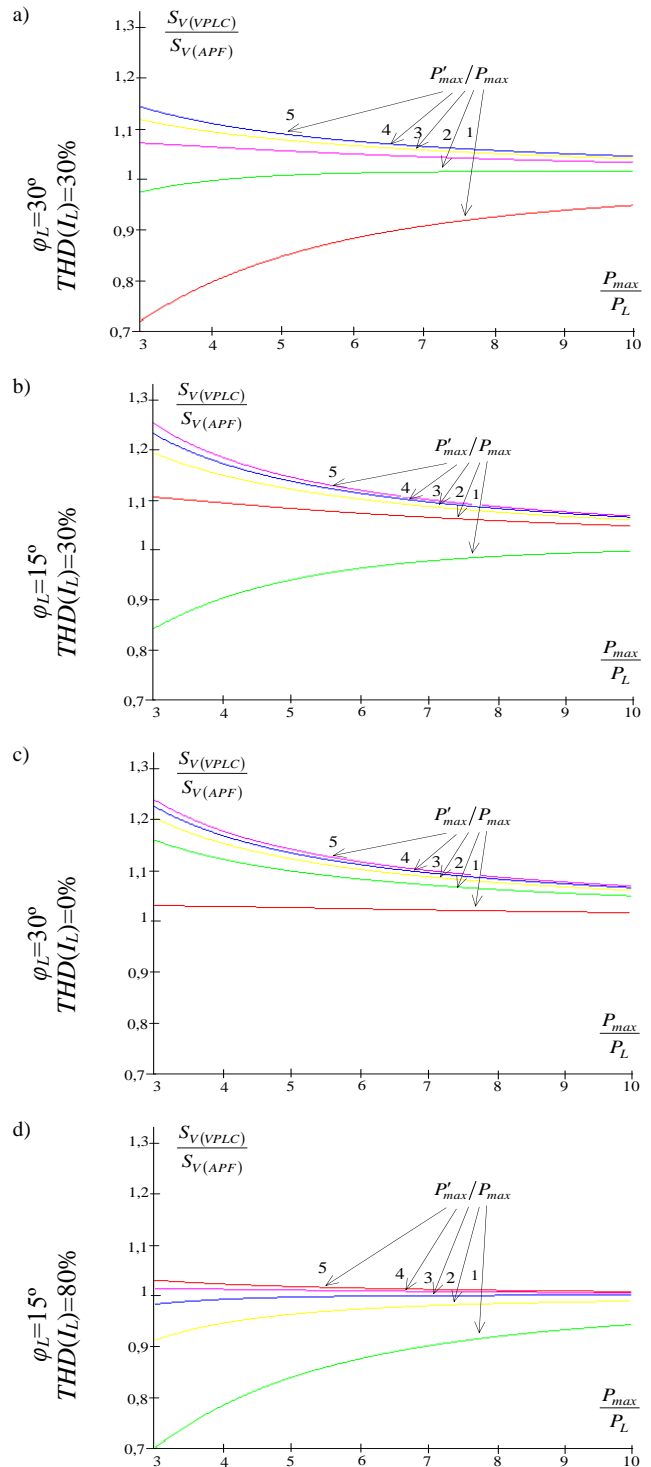
Fig. 5. The results obtained on the base (12) for different $\varepsilon = P_{max}/P_L$, φ_L, $THD(I_L)$, as well as different inductances L_S and L'_S ($P'_{max}/P_{max} = L_S/L'_S$).

In addition to that, deformations in load current, characterized by number of compensated harmonic N and $THD(I_L)$ influence energetic properties of both arrangements. The compensation of the higher harmonics in VSPLC load

current, does not require any changes in voltage u$_V$. This is different thatn in APFs. In APFs, a component in the compensating current, that is responsible for compensation of higher harmonics (which flows through coupling inductance L'_S) is determined by the another component in voltage u$_V$. This tends to lead to growth of its effective value. It can be concluded, that VPLC is desirable for loads with large harmonic content, e.g. for rectifiers with capacitive load

A comparison of filtration quality, that can be achieved with VSPLC, and classical APF provides a create view of the difference between the two solutions. An instantaneous power theory was used to obtain compensating currents. All tests were made for both RL and RC rectifier loads (Fig.6). By looking at obtained curves, we it can be said that controlled voltage source in parallel connection to the network poses better filtration properties . The filter is resistant to the shape of a load current. This is possible because distorted load current compensating components don't need to be extracted. However, in classical APF filtration the quality depends on determination accuracy of the compensating components and ability of the inverter to shape them.
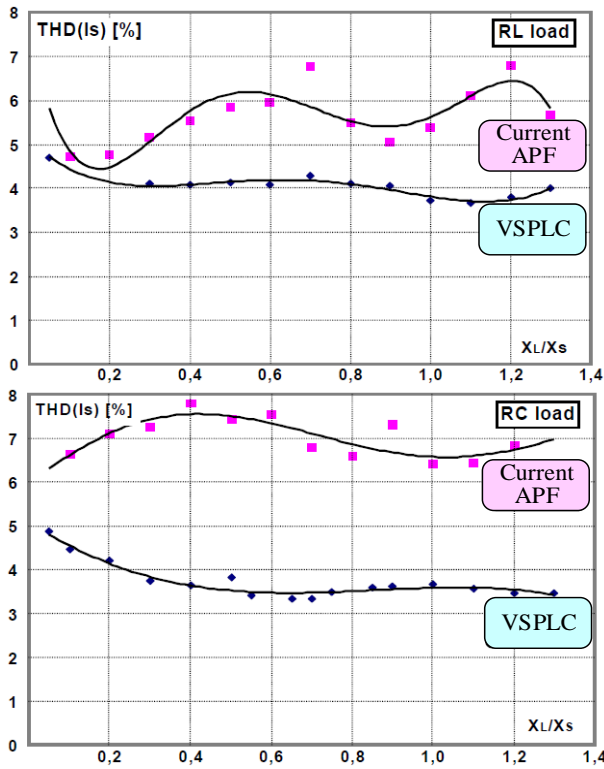

Fig. 6. Comparison of filtration properties of classical, current APF system and investigated VSPLC

IV. FOUR-LEVEL VSPLC

A. Cascade 4-level VSC system - voltage source to VSPLC

Multilevel converters are a well fitted solution for utilization in described VSPLCs, because they can produce output voltage with large number of steps [9,10].

Fig.7 presents proposed 4-level converter- a series connection of the three one-phase converter bridges (T1-T4, T1'-T4', T1''-T4'') with the 3-phase converter bridge (T5-T6; T5'-T6'; T5''-T6''). The converter works in 3- and 4-line networks. in 4-line networks, the DC supply

capacitor in the three-phase converter bridge is divided to create zero point. One can see that in the converter' output voltage is a geometrical sum of voltages (for phase L1) on converter VSC 2L and VSC 3L1, respectively. Fig.8 shows results of the experiment. The converter uses a multilevel carrier based PWM, whereas N-level converter has a set of N-1 triangular carrier waves with the same peak-to-peak magnitude and frequency.
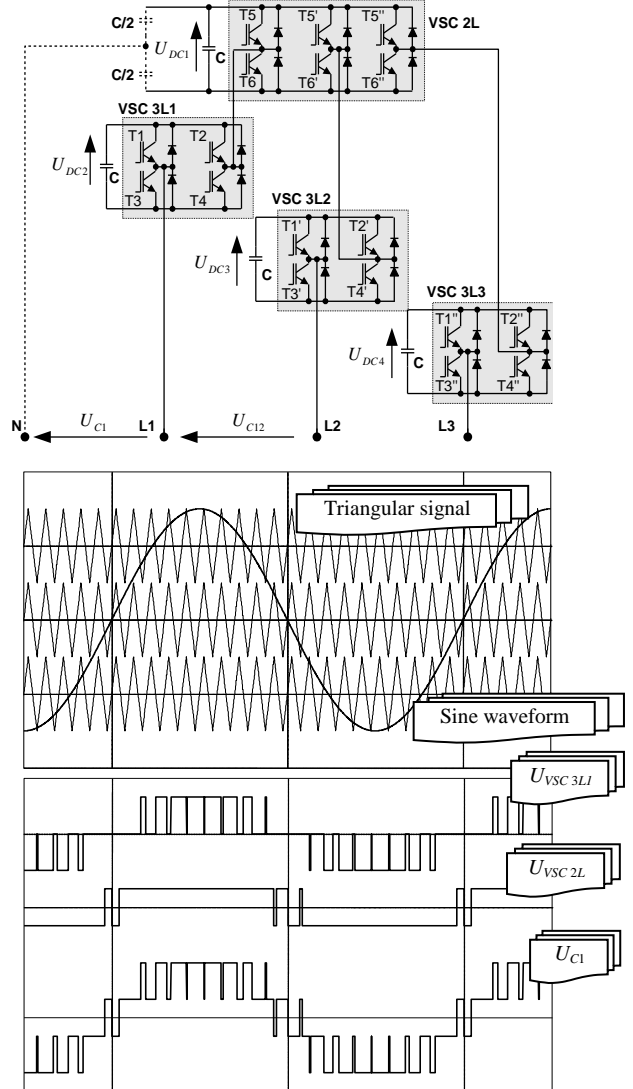

Fig. 7. From the top - topology of the 4-level cascaded VSC system, below the synthesis of the phase voltage
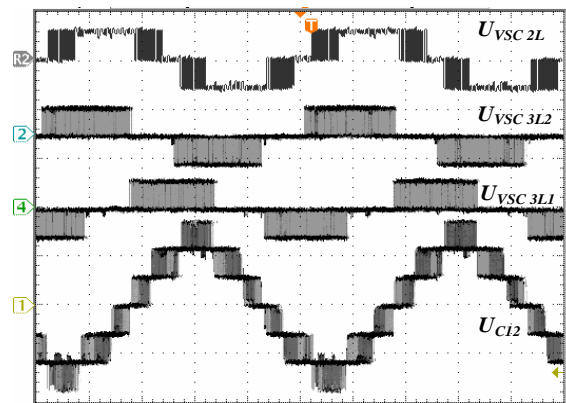

Fig. 8. Multilevel VSC – experimental results (U – 500 V/div, time – 4ms/div).

B. VSPLC control algorithm

Control algorithm in the multilevel VSPLC can be divided into two major parts. First one, see Fig.9, determines voltage $u_{V(REF)}$. The amplitude of voltage $u_{V(REF)}$ equals the nominal amplitude of the supplying voltage u_S. The angle γ_0 enables the flow of required energy thru the series impedance Z_S to the load.

When the actual power supplied from source is greater than the load demand (γ_0 to large), the surplus portion can be absorbed by the VSC increasing total DC link capacitor voltage. When the actual source power is less than the load demand (γ_0 to small), the total DC link capacitor voltage decreases. In. this case angle γ_0 is determined based on the energy balance on the DC links.

If angle γ_0 is determined properly, the u_{DC} voltage is constant, and the average active power exchanged between VSC and network equals 0 (assumed that losses related to commutation are diminished). A PI controller regulates the total DC link capacitor voltage. The controller uses the error between the reference u^*_{DC} and the total DC voltage u_{DC} as a feedback signal.
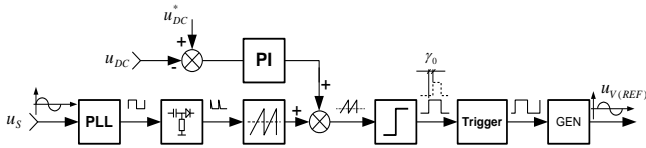

Fig. 9. Multilevel VSPLC – $u_{V(REF)}$ determination (phase L1).

As noted abover, changes of the γ_0 angle impact the real power absorbed or supplied by the VSC, thus the total DC link capacitors voltage can be regulated. However, to avoid the problem of unbalanced voltages on the selected capacitors (u_{DC2}, u_{DC3}, and u_{DC4}) the control algorithm should be equipped with additional part (Fig.10). It secures constant and balanced voltages u_{DC2}, u_{DC3}, and u_{DC4} as a result of variable switching strategy of the transistors [11].

Changeable switching strategy can be established by adding a constant component to the triangular carriers (this does not change converter's output voltages and currents). The constant component can be obtained by comparing the reference voltage, in phase L1 - u^*_{DC2}, and the actual measured value, during phase L1 - u_{DC2}. The constant component, obtained with this method shifts the triangular waves and changes switching strategy to equalize the DC link voltages. Finally the load voltage stabilizes at the reference value by means of a closed-loop control error between the u_V and the reference voltage $u_{V(REF)}$.
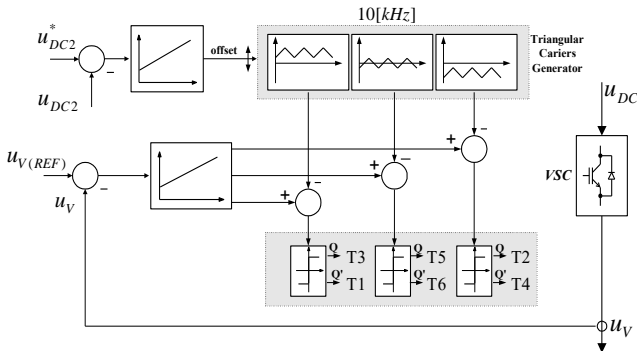

Fig. 10. Multilevel VSPLC – balancing DC voltages (phase L1).

V. EXPERIMENTAL RESULTS

A 4-level VSPLC model, with parameters presented in Table I was developed to verify the theoretical investigations. DC link voltages were controlled to be even $u_{DC1}=u_{DC2}=u_{DC3}=u_{DC4}$ and the output VSC's a Γ passive filter was implemented.

TABLE I.   EXPERIMENTAL PARAMETERS OF VSPLC

Name	Value
Supply voltage	80 [V]
DC link reference voltage	70 [V]
Inductance L_S	5.4 [mH]
Γ filter inductance L_f	0.3 [mH]
Γ filter capacitance C_f	18 [μF]
DC link capacitance C	2200 [μF]
Switching frequency	10 [kHz]

Fig.11 and Fig.12 show experimental waveforms, during multilevel VSPLC's steady state operation, for non-linear load (a six pulse rectifiers with resistive-inductive and capacitive load). As one can see from those figures, the load current contains a large in amount harmonics due to the nonlinear load; however, the source current is almost sinusoidal. Additionally, Table II shows the supply and the load current THD coefficients.
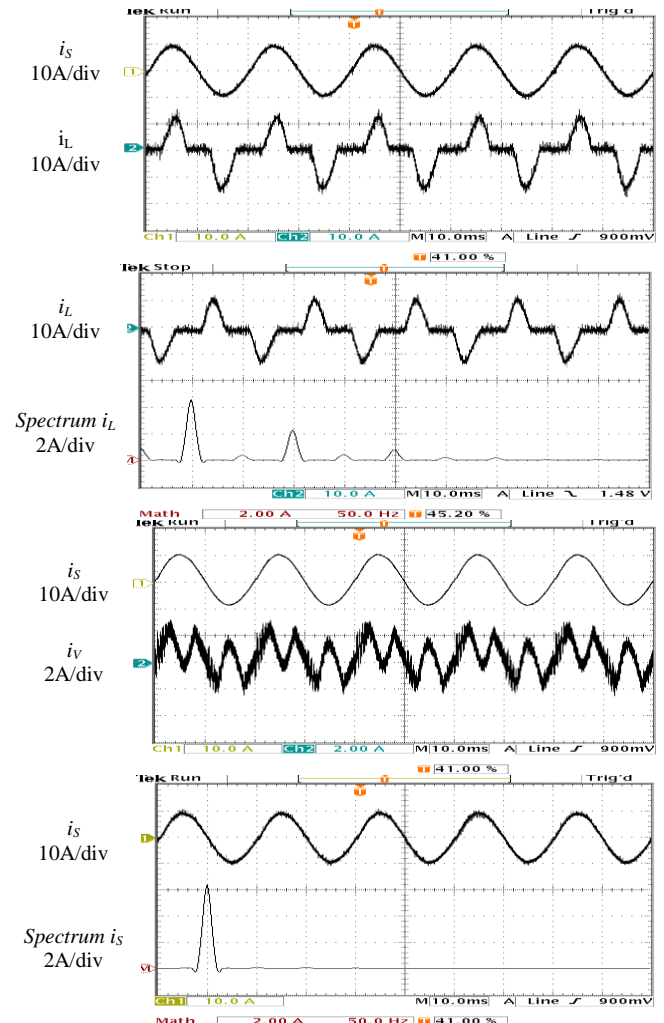

Fig. 11. VSPLC experiment for first nonlinear load (6-pulse rectifier – capacitive RC load) P_L=1 [kW], (Δt = 10 ms/div)
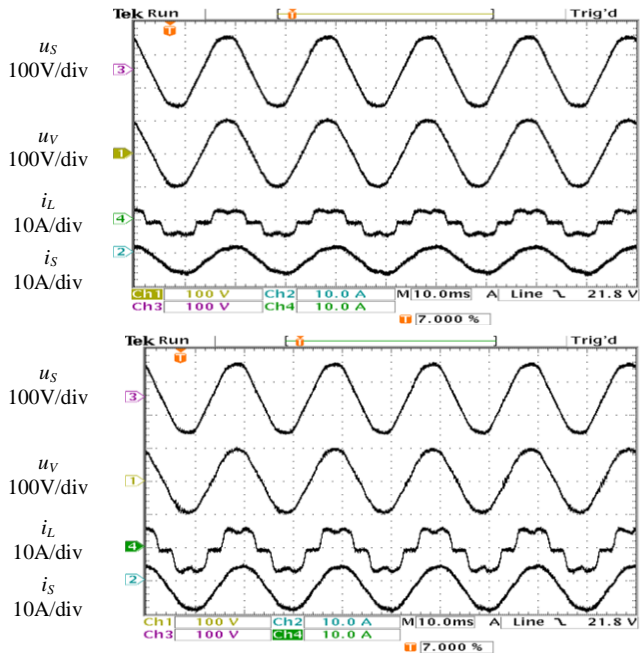
Fig. 12. Experiment for second nonlinear load (6-pulse rectifier – *RL* load): from the top P_L=0.8 [kW], from down P_L=1.2 [kW], (Δt = 10 ms/div).

TABLE II.   THD COEFICIENTS

Six pulse rectifier	Value	
	i_S	i_L
RL load	3,3	25
Capacitive *RC* load	3,5	45

In the tested model, load active power P_L = 0.8 kW generates φ_S = 9° - angle between the supply current and voltage and thus the input PF is 0.98. Increasing voltage u_V amplitude, leads to full compensation of the load reactive power and the unity power factor. While the u_V voltage amplitude is 1.3% higher than source voltage u_S (Fig.13), it is within the range proposed by the European standard EN50160 (limits voltage increases to 10%).
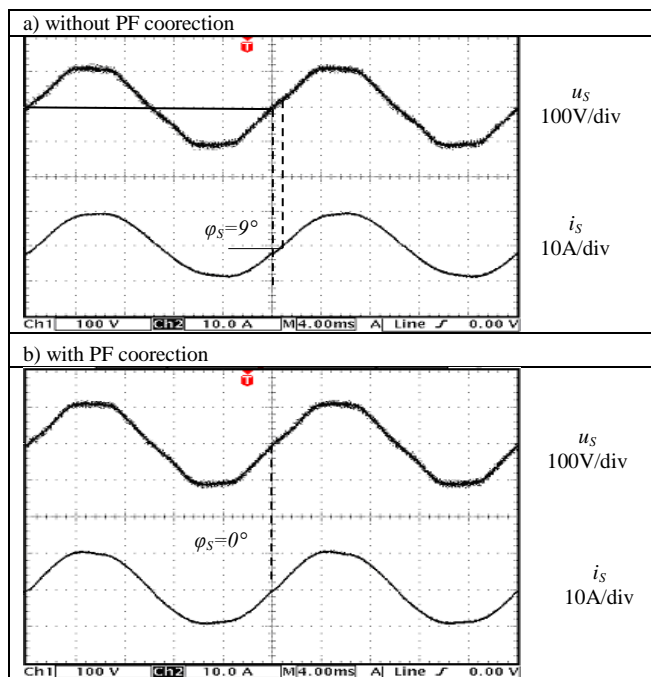

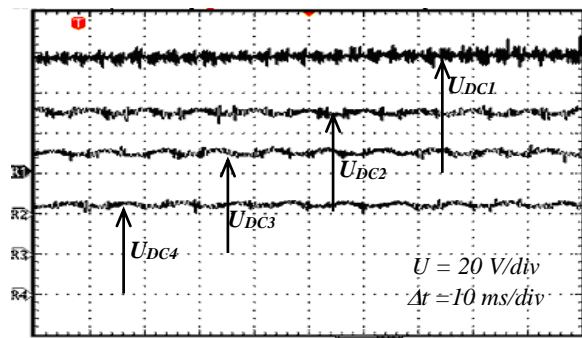Fig. 13. VPLC – input power factor correction

Fig. 14. Fig.10 Multilevel VSPLC - DC link voltages.

Fig.14 shows that proposed algorithm for balancing DC voltages works properly in situation of the non-linear load, voltages on the DC capacitors.

VI. CONCLUSIONS

Paper discusses 3-phase multilevel Voltage Source Power Line Conditioner (VSPLC). A ccrucial advantages of VSPLC systems, in comparison with APF systems are: very good filtration proprieties for any kind of nonlinear loads; better energetic properties especially in case of nonlinear loads with large number of produced harmonics, possibility of use of simple network inductance L$_S$, matched only with regard of basic frequency 50/60 Hz. The VSPLC four-level cascade based voltage converter was developed. A down scale hardware model has been developed to verify properties of the proposed conditioners. After experiments one can say that:

- − VSPLC is free from higher harmonics source current, even with strongly deformed load current; source current wave shape;
- − VSPLC is capable of compensating reactive power. and unbalanced load current

REFERENCES

[1] F. Peng, H. Akagi, H. Nabae: "Compensation characteristics of the combined system of shunt passive and series active filters," IEEE Trans. on Industry Applications, 1993, Vol.29, No.1, pp.144-15.

[2] R. Strzelecki, H. Supronowicz: "Power factor in AC supply systems and improvements methods," Publishing house of the Technical University of Warszawa, 2000.

[3] H. Akagi, E.H. Watanabe, M. Aredes: "Instantaneous Power Theory and Applications to Power Conditioning", Wiley-IEEE Press, 2007

[4] L. T. Moran, P. D. Ziodas, G. Joos, "Analysis and design of a novel 3-F solid-state power factor compensator and harmonic suppressor system", IEEE Trans. on Industry Applications, vol. 25, pp.609-619, July/August 1989.

[5] L. Moran, E. Mora, R. Wallace and J. Dixon, "Line conditioning system with simple control strategy and fast dynamic response," IEE Proceedings - Generation, Transmission and Distribution, vol. 142, no. 2, pp. 128-134, 1995.

[6] R. Strzelecki, J. Rusiński, G. Benysek: "Voltage source power quality conditioner, " Electromagnetic phenomena in Nonlinear Circuits - EPNC 2002, XVII Symposium. Leuven, Belgia, pp. 179-182, 2002

[7] Y.H. Song, A.T Johns (1999). Flexible AC Transmission System*s*. IEE Power and Energy Series 30, IEE, 1999

[8] A.B. Williams, F.J. Taylors, "Electronic Filter Design Handbook", McGraw-Hill, 1988.

[9] J. Rodriguez, Jih-Sheng Lai and Fang Zheng Peng, "Multilevel inverters: a survey of topologies, controls, and applications," in IEEE Trans. on Industrial Electronics, vol. 49, no. 4, pp. 724-738, 2002.

[10] H. Akagi, "Multilevel Converters: Fundamental Circuits and Systems," in Proceedings of the IEEE, vol. 105, no. 11, pp. 2048-2065, 2017

[11] R. Strzelecki, G. Benysek, J. Rusiński, E. Kot.: "Analysis of DC Link Capacitor Voltage Balance in Multilevel Active Power Filters," EPE'01-Graz.